Space-borne Ka-Band Across-Track SAR Interferometer

Christoph Schaefer[(1)], Michael Völker[(1)],
Paco López-Dekker[(2)], Marwan Younis[(2)],
Elena Daganzo-Eusebio[(3)] and Michael Ludwig[(3)]

[(1)] Astrium GmbH, 88039 Friedrichshafen, Germany
Email:Christoph.Schaefer@astrium.eads.net

[(2)] Deutsches Zentrum für Luft- und Raumfahrt,
PO Box 1116, 82230, Wessling, Germany
Email: Francisco.LopezDekker@dlr.de

[(3)] European Space Agency-ESTEC, Noordwijk, Netherlands
Email: Elena.Daganzo-Eusebio@esa.int; michael.ludwig@esa.int

ABSTRACT

The results of an ESA study concerning a future Ka-band SAR mission and instrument concept are reported. One aim of the study has been to explore the feasibility of a future single-platform, across-track interferometric SAR instrument with HRTI-3 performance of its Digital Elevation Model data product. The possibility of accommodating an interferometric instrument with electrically large across-track baseline on a single platform is a unique opportunity to avoid the temporal decorrelation of repeat pass concepts at lower carrier frequency. On the other hand, sensitivity requirements of space-borne instruments demand the use of electrical large antennas; these inevitably require Digital Beam Forming capabilities. Hence these become a fundamental part of the present design issue.

An instrument architecture is presented which minimizes antenna masses attached to the ends of its long boom, and which constrains the installation of electrically active units or components to the satellite body. These features support a very stable instrument while keeping implementation complexity moderate. To achieve this, Digital Beam Forming techniques are applied both in elevation and azimuth direction.

The SAR and InSAR performances of the instrument concept are reported. The assessment of the expected In-SAR performance requires a full account of all mechanical, thermal, and electrical errors which persist after the proposed calibration measures. These include an innovative multi-squint procedure which allows to calibrate mechanical oscillations of the boom from the SAR data itself, in the on-ground processing stage. The procedure is related to motion-compensation correction methods used in airborne SAR. While the presented instrument concept is geared towards high-resolution data products with only moderate scene sizes, optional instrument architectures can also be considered which offer wide swaths at reduced resolution. It is concluded that Ka-band offers a number of promising instrument alternatives for future interferometric SAR missions with rewarding performances.

INTRODUCTION

Background And Objectives

The motivation for conceiving a SAR mission at Ka-band results from the small wavelength (8.4mm @ 35.75GHz). The impact of small wavelength is twofold. From an application point of view, low penetration into ground supports an accurate measurement of e.g. snow and vegetation height. Also precipitation is visible at Ka-band, which can be either a nuisance or an advantage, depending on the targeted application.

From an implementation point of view, compact SAR system designs seem feasible. This is particularly appealing if considering a single-pass, single-platform interferometric SAR instrument (InSAR), since electrically large baselines become feasible with booms of reasonable lengths. An across-track InSAR of such build with a targeted height accuracy of its Digital Elevation Map (DEM) of ~2m has already been proposed [1]. Mission objectives are high-resolution, 3-D security and monitoring services over land or sea with limited swath width in the order of 10-20 km as well as medium resolution environmental monitoring (e. g. ice volume) with wide swath in the order of 50 km.

With [1] as the starting point, an ESA-funded study is being pursued by a consortium constituted of Astrium Satellites, Astrium Services and DLR-HR. The aim of this paper is to briefly report the instrument concept developed in this context, and to highlight the significant contribution of Digital Beam Forming (DBF) techniques in this context.
In section 2, the paper introduces the preferred architecture for an across-track InSAR operating at Ka-band. Section 3 presents expected SAR and InSAR performances.

Challenges

There are a number of particular challenges associated with a Ka-band InSAR. At given mechanical baseline, for best interferometric performance, instrument phase error must be minimized. This requires appropriate system- and instrument-level calibration procedures. The electrical and mechanical/ thermal stability becomes a critical issue if we wish to provide a baseline of ~ 20 m at a wavelength of < 1 cm. Oscillations and thermal distortion of the boom must be compensated, and potential reflector antenna defocusing and mispointing must be avoided.

A second issue arising with any compact spaceborne instrument is sensitivity. The amount of transmit power that can be supplied by technology today is limited. To achieve a Noise-Equivalent Sigma-Zero of e.g. NESZ<–15dB, an effective aperture area of the receive antennas of >5m² is required. This corresponds electrically to apertures of >70m² at X-band or >220m² at C-band. Comparing this with the C-band phased array antenna of the forthcoming Sentinel-1 instrument with an area of 10m², it is clear that we are presently dealing with electrically extremely large antennas. This inevitably entails the need for DBF techniques. The scan-on-receive technique in elevation (SCORE) sweeps the high-gain pencil receive beam across the swath; a static beam would not be able to illuminate the full swath width. The multiple aperture processing scheme (MAPS) is a DBF technique applied in azimuth; it allows to lower the PRF and widen the available swath. MAPS in our case supports a 2 transmit- / 2 receive-antenna configuration with several implementation advantages.

INSTRUMENT ARCHITECTURE

Design Considerations

The requirement of instrument compactness will inevitably limit the sensitivity of a spaceborne Ka-band SAR instrument, forcing the designer to choose between a wide swath / low resolution instrument architecture, and a high resolution / narrow swath architecture. The latter has been selected presently, with the aim of providing a large number of looks for interferometric averaging and of achieving challenging HRTI-3 level DEM height accuracy. High-gain reflector antennas and swath selection by platform roll are proposed. This design choice keeps antenna complexity moderate. Like in [1], the transmit (TX) antenna is equipped with a single feed, while each receive (RX) antenna provides a multi-feed array (MFA) for SCORE elevation beam scan within a single swath.

Two potential architectures are shown schematically from the bore-sight perspective in Fig. 1. TX antennas are orange, RX antennas are blue. The architecture on the left is the baseline architecture, while the one on the right is a hybrid architecture which can provide both across-track and along-track interferometry; the latter for Moving Target Indication with as many as four virtual phase centers. The along-track baselines of the hybrid architecture with asymmetric mount of its TX antennas can also be obtained by mechanically tilting the baseline architecture around its bore-sight axis (platform with small pitch angle).

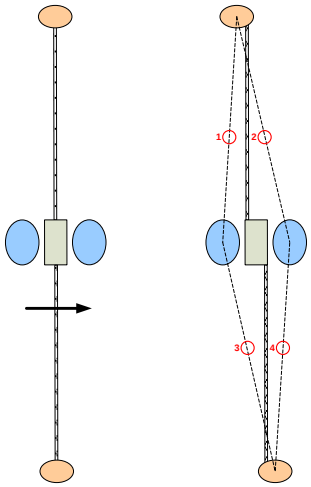

Fig. 1: Schematics of baseline architecture (left) and hybrid architecture with four virtual phase centers (right)

In these architectures, two TX antennas are provided at the ends of the boom. Since the TX reflectors are quite small (each 2 × 0.4 m²), the mechanical requirements on the boom are minimized. The orange TX antennas are actually just passive, primary antennas; secondary antennas with active feeds are mounted on the platform. This approach avoids laying RF waveguides along the deployable boom, and minimizes calibration efforts and electrical losses in these waveguides. The secondary TX antenna with its active feed is firmly mounted on the platform where it is under tight thermal control.

The full baseline is spanned by two identical half-booms of length ~ 10m. They are proposed as hinged or telescopic constructions for stowage, without electrical functions. The mechanical stability of these booms is of eminent importance for the final instrument phase error, particularly if the need for roll manoeuvres of the platform is kept in mind.

The two large RX antennas (each 2 × 2 m²) are connected to the sides of the platform using hinges, allowing them to embrace the platform in stowed mode and to unfold during deployment in orbit. Their respective MFAs are firmly attached to the sides of the platform, establishing an offset-parabolic reflector illumination geometry. All active Ka-band electronics are thus directly and firmly integrated with the platform, providing a promising baseline for tight thermal control and electrical stability.

Each TX antenna is supported by its own Extended Interactive Klystron (EIK) as RF power source. A peak power of ~ 3500 W, depending on required bandwidth, is state-of-the-art performance [2]. The dual TX approach has the advantage of doubling the available RF transmit power of the instrument without requiring power combiners with RF losses and potential multipaction problems. This approach also seems favourable under device failure aspects.

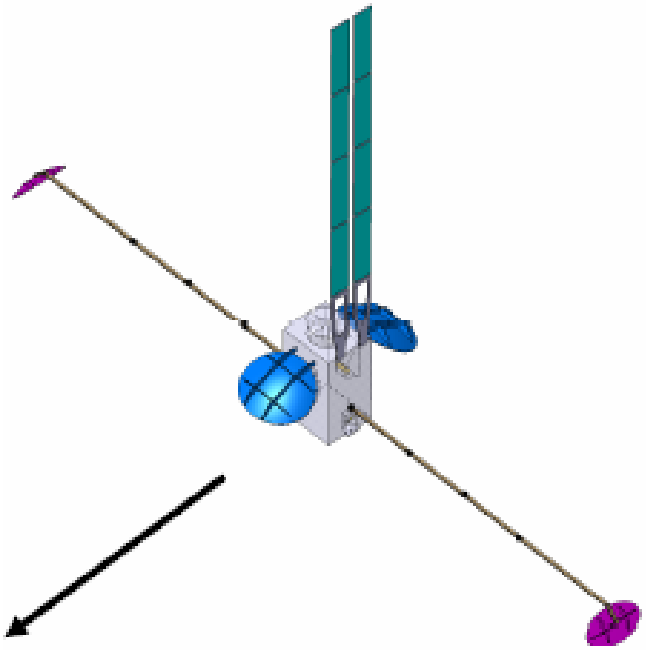

Fig. 2: True-scale illustration of deployed baseline instrument

DIGITAL BEAM FORMING FUNCTIONS

SCORE and MAPS are the two digital beam forming techniques required in this concept. A useful SCORE reference is [3].

MAPS operates in the azimuth/ Doppler domain, combining SCORE-processed signals received by multiple along-track apertures. MAPS usually requires no on-board processing. MAPS×N may be viewed from a sampling perspective [4] or from a beam-forming, spectrum reconstruction viewpoint: the RX antenna is made longer than required for classical SAR, in order to view a reduced instantaneous Doppler bandwidth and thus to admit low PRF (often required to increase swath width) and to increase sensitivity, but is broken down into N subapertures to gain azimuth scan and multi-beam capability; during on-ground processing, the narrow azimuth beam of the long antenna is swept in the Doppler domain using the separately recorded subaperture signals, thereby reconstructing the full signal spectrum.

In our case, the lower and upper TX antennas are pulsed in turn ("toggled mode"), interlacing the recording of the raw data corresponding to the lower and upper SAR images. These two SAR images are later used to produce the interferogram. The toggling effectively halves the PRF which is available for the generation of each image. The two RX antennas are then applied in a MAPS × 2 mode to achieve the same swath width as would be feasible in an architecture not requiring toggle.

The placement of the platform between the RX antennas facilitates stowage and implementation. The along-track gap introduced between the two RX antennas needs to be compensated by increasing the burst length of the toggled pulse transmission: e.g. each TX antenna sends 2 pulses (at instrument PRF) before switching to the other and then pausing for 2 pulses.

Of course, besides compensating for the introduction of toggle, the second RX antenna is also required to gain 3dB of sensitivity.
It should be noted that since loss of sensitivity is to be avoided, azimuth beam width, instrument PRF and antenna physical along-track separation must be consistent.

Transmit Receive Phasecentre sampling positions

The inset of Fig. 3 illustrates the along track position of the Tx/Rx phase centres for a sequence of pulses with burst length of 2. A very long PRI = 0.8 ms (low PRF) is used for illustrating the physical instrument positions only. PRI dependency of the *along track* sampling positions is plotted – more details are shown in Fig. 4.

Within the 1st (green) and 2nd (red) *instrument pulse (PRI)* the upper antenna (Top) transmits and the return is measured using the Fore (solid) and Aft (dashed) receive antennae. Within the next two instrument PRIs (blue, yellow) the lower (Bottom) transmit antenna is used. The sequence repeats with the 5th instrument PRI.

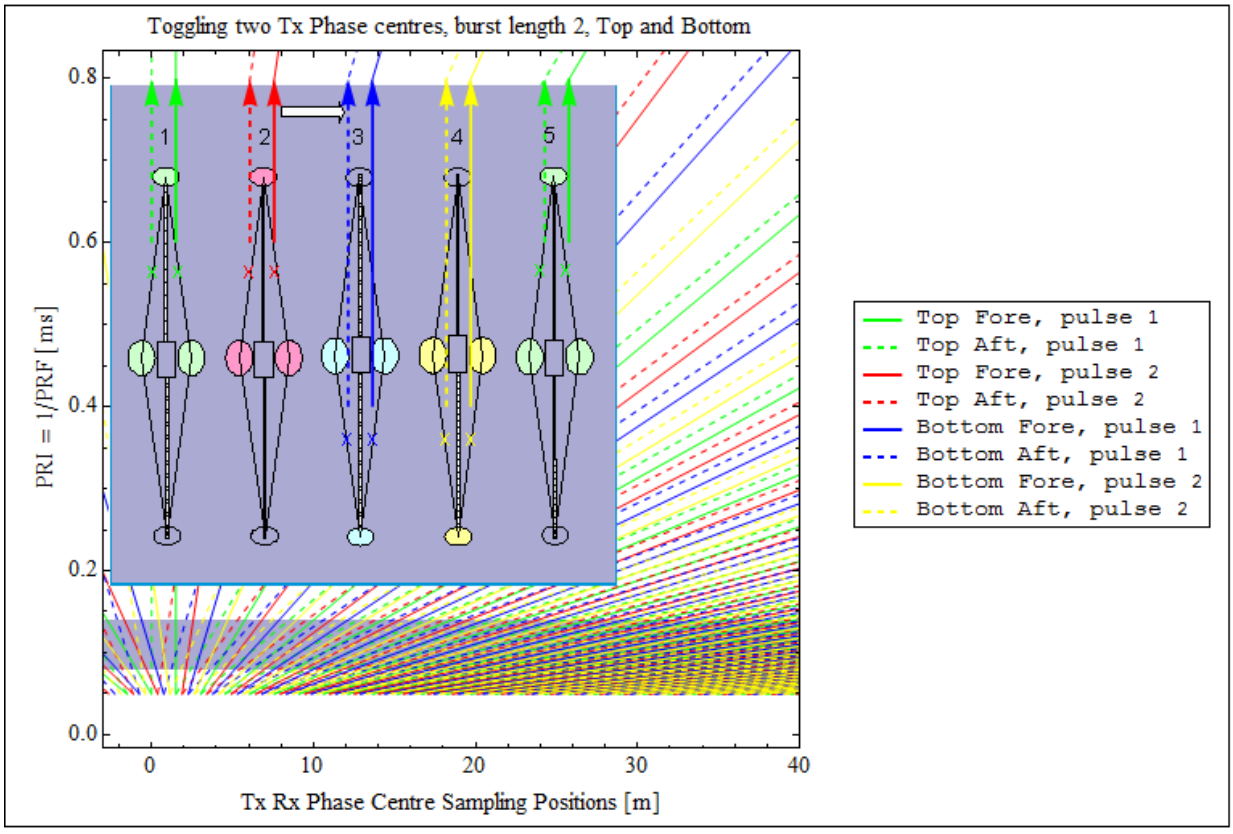

Fig. 3: Sampling Position of upper and lower TxRx phase centres depend on PRI. Details see text.

The along track sampling positions of the upper (Top) and lower (Bottom) phase centres of Fig. 3 are extracted and the useful instrument PRI range is enlarged in Fig. 4. For across track interferogram generation both sets of sampling positions are used for processing of a contributing SAR image. Therefore both sets need to have “proper sampling” for themselves. The useful region of more or less regular sampling corresponds to 7.1-12.5 kHz *instrument PRF*.

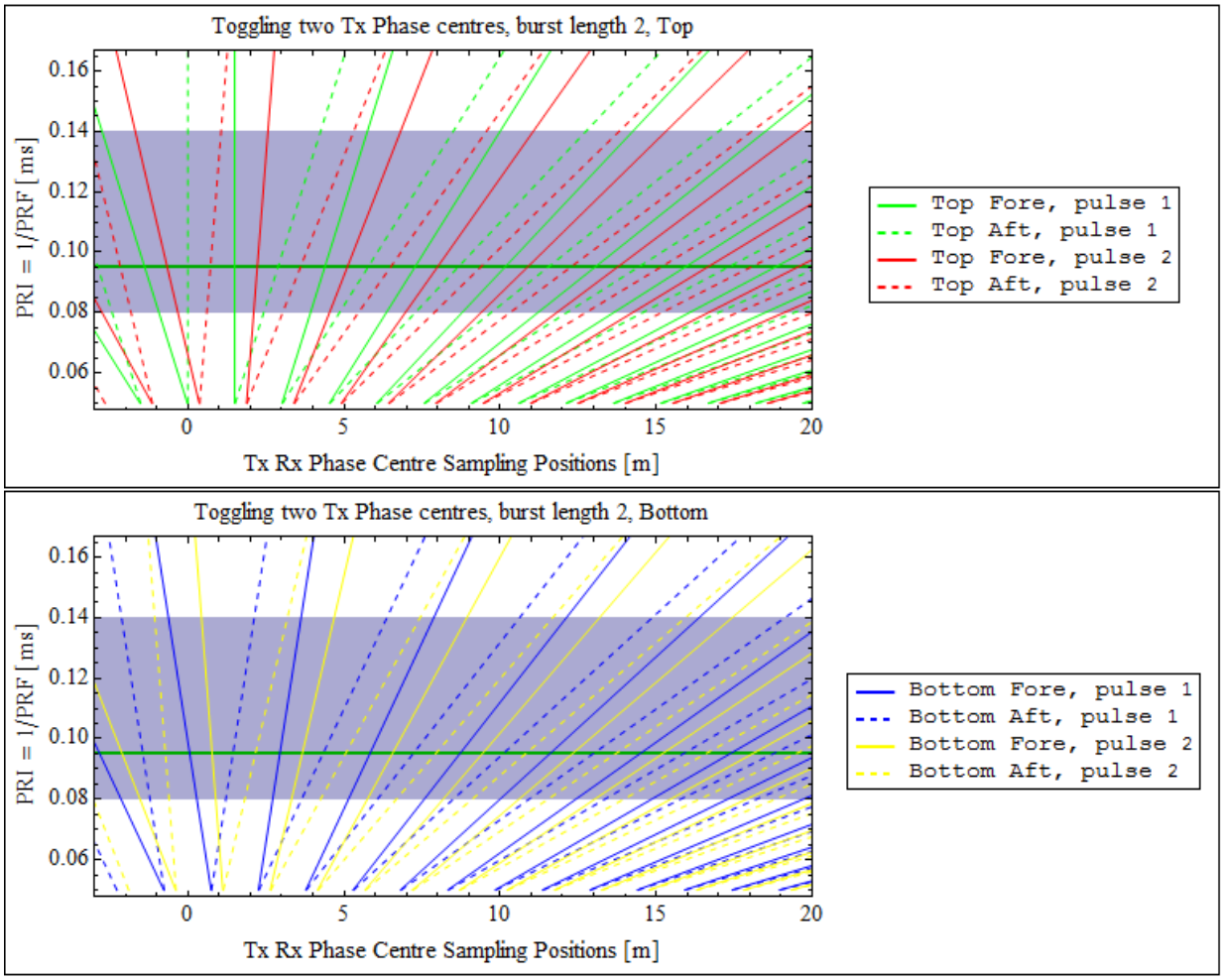

Fig. 4: Sampling Position of upper and lower TxRx phase centres plotted separately. Beside (mechanical) offset, the position depends linearly on instrument PRI. The useful region of more or less regular sampling is highlighted: the *instrument PRF* range corresponds to 7-12.5 kHz. The green horizontal line depicts the nominal *instrument PRF* of 10.5 kHz.

Fig. 5 shows the sampling for simple toggling of upper and lower transmit phase centre – i. e. burst length 1. This "sequence" allows to extend the useable *instrument PRF* to below 7.6 kHz and within 13.3-15.4 kHz. A three pulse burst length does not significantly extend the useful PRF range beyond the variants as of Fig. 4 and Fig. 5.

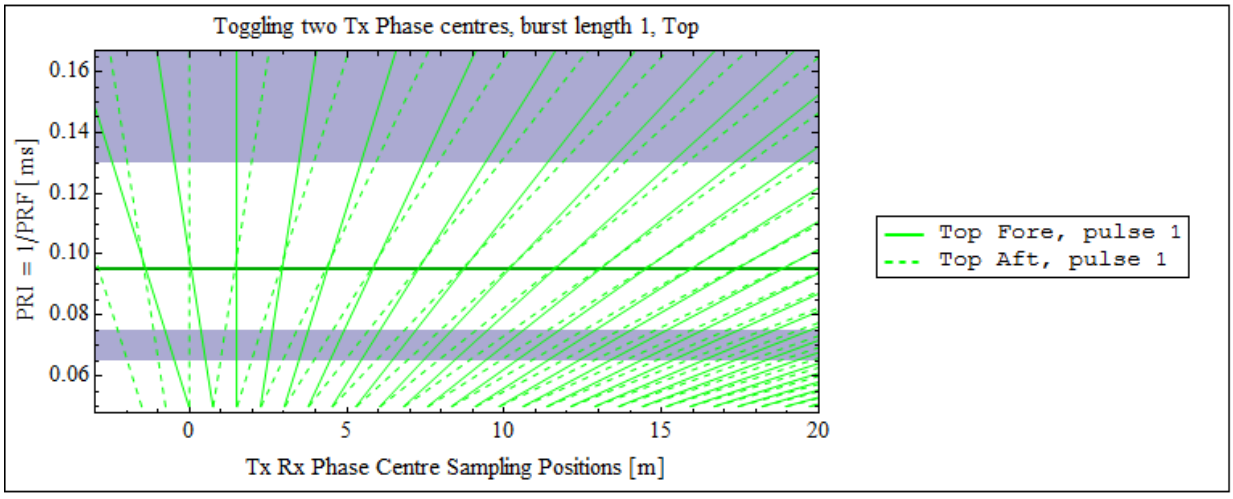

Fig. 5: Sampling Position of upper TxRx phase centres for burst length of 1 i. e. toggling upper and lower Tx antenna. This mode extends the useful instrument PRF range beyond the two pulse burst mode (Fig. 4).

PERFORMANCE

SAR Performance

The performance of the baseline architecture has been evaluated using DLR's SAR performance analysis tools. These results form the basis for the XTI performance analysis. The radiation patterns of the reflector antennas were calculated using GRASP with the simplification that the feed pattern was approximated by a simple tapering function.

A rough system optimization was carried out, with the main goal of achieving a 12 km minimum swath width. This implied choosing the lowest possible Nyquist-compliant PRF satisfying the condition of aligning the transmit events with the swath returns. Considering the MAPSx2 mode and transmit toggling, this is achieved setting the system PRF to approximately 10 kHz.

Note that image reconstruction under MAPS is optimized for a fixed combination of PRF and antenna separation, which implies that (roughly) the same PRF must be used independently of the incidence angle.

Fig. 6 shows the calculated Noise Equivalent Sigma Nought (NESZ) as a function of ground range (from nadir) and incidence angle, and including 4 dB of two-way atmospheric attenuation. The ripple is introduced by the multiple SCORE receive beams, while the single feed and fixed transmit pattern causes the sensitivity loss at the edges of each swath shown.

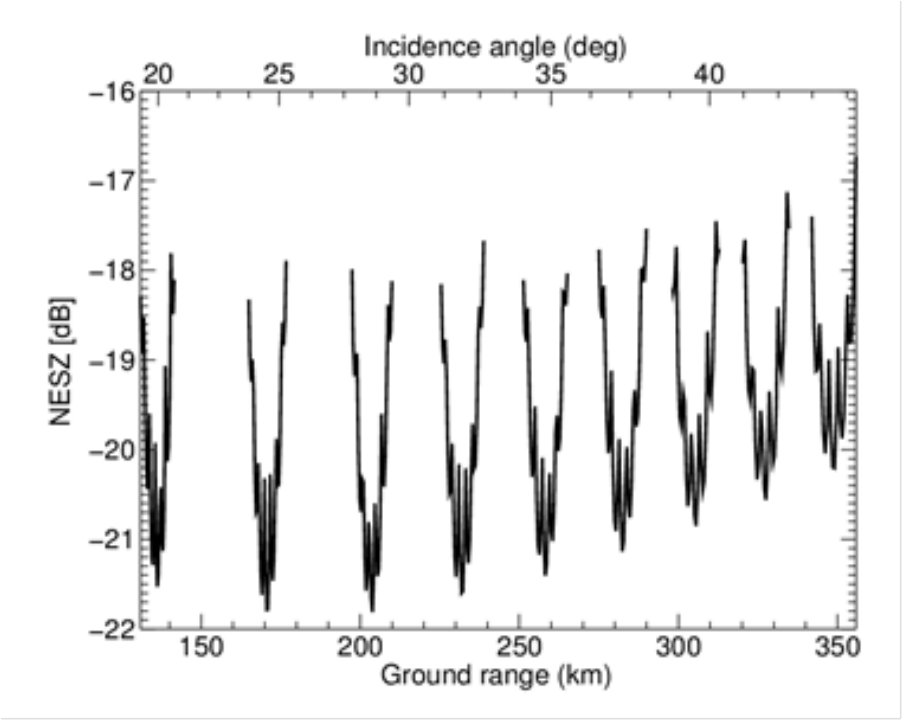

Fig. 6: Calculated NESZ as a function of ground range (bottom axis) and incidence angle (top axis) assuming a ground range resolution 2 m.

The feed tapering was optimized in order to maximize the NESZ for far range swaths, for which the swath widths are timing limited. The consequence is that, for near range swaths, the achievable swath width becomes antenna pattern limited.

InSAR Performance

The cross-track interferometric performance estimation follows the methodology used in the performance analysis of TanDEM-X [5]. The performance evaluation considers noise-like decorrelation sources (i.e. error sources that can be mitigated by multi-looking) and systematic errors. The following decorrelating effects are considered: thermal and quantization noise assuming an 8:4 BAQ scheme; range and azimuth ambiguities, which are treated as an uncorrelated interference signal; and volume decorrelation. For geometric decorrelation due to spectral shift it is assumed that an ideal common-band filtering is applied, so that there is no coherence loss but, instead, only a loss of effective resolution and, therefore, a reduced number of looks. Given the single-pass nature of the mission, there is no temporal

decorrelation term. An additional general decorrelation term is included to model residual coregistration errors and differences between the two interferometric channels. For the results presented, this term is set to 0.98, which is then the maximum achievable coherence.

The random component of the phase error is derived from combining the coherence and the number of looks and is subsequently scaled to height by the height of ambiguity. For the 20 m baseline considered, despite the short wavelength, the height of ambiguity ranges from approximately 100 m for the near range swaths considered, to above 200 m at far range.

Fig. 7 shows the predicted relative point to point error as a function of ground range and incidence angle, using as an input the previously discussed SAR performance. The results shown correspond to 90% confidence point to point relative errors, which is equivalent to $2.33 \cdot \sigma_h$, where σ_h is the standard deviation of the relative height error. A multi-looking window corresponding to the HRTI-3 standard 12x12 m^2 resolution has been used, yielding 60 looks for all ground range positions. The different curves correspond to a variety of surface types, characterized by the normalized radar cross-sections reported in [6].

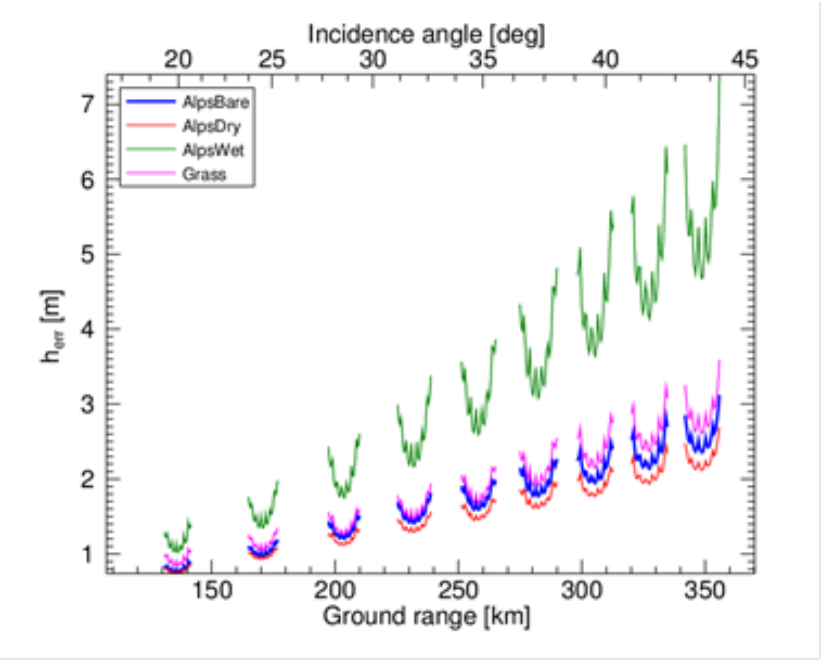

Fig. 7: 90% confidence point to point height error as a function of ground range and incidence angle; two-way atmospheric loss of 2 dB assumed.

There are three main effects modulating the performance. This first is the SNR, which is better at close range due to better NESZ and, to some extent, the steeper incident angle. As expected, the performance is also strongly dependent on the surface type. The second, and very important, effect is the range dependence of the height of ambiguity, which justifies about a factor of 2 difference between the near and far range expected relative errors. The last is the ground range resolution, which improves for large incidence angles, therefore increasing the number of available looks at far range. The results shown are within the 2 m target error set by the HRTI-3 standard for the surface types shown for incidence angles below 35 to 40 degree.

DISCUSSION

In this paper we present an overview of the design of a Ka-Band single-pass InSAR system. We propose an unconventional approach, with two toggling transmitting antennas. This solution is a key to the feasibility of the system, allowing the use of light-weight and, therefore, longer booms, which are critical to achieve the desired interferometric sensitivity. It also significantly reduces the total mass of the system compared to a solution featuring two large receive antennas. Careful mechanical design is still required to guarantee the stability of the long boom, particularly after rolling the platform when addressing a new swath. The main disadvantage of transmitter toggling is the higher required PRF. The problem is solved by the use of digital beam forming methods.

The presented analysis has focussed on a narrow swath application with a relative height error performance at HRTI-3 level. This performance requirement is met for most types of terrain. With an alternative architecture which provides

antennas with beam scan capability in elevation and which employs ScanSAR modes with accordingly reduced performance, it is expected that a swath width of ~50 km can be achieved.

ACKNOWLEDGMENTS

The authors of this paper acknowledge the valuable and detailed contributions of the complete ESA review team including mechanical, thermal, antenna as well as system design disciplines.

REFERENCES

[1] Ludwig, M.; D'Addio, S.; Engel, K.; Aguirre, M.; Angevain, J.C.; Saenz, E.: *"A Spaceborne Ka-Band SAR Interferometer Concept based on Scan-on-Receive Techniques"*, EUSAR 2010, June 8-10, Aachen, Germany

[2] Roitman, A.; Viant, M.; Nilsen, C.; Cattelino, M.; Berry, D.; Steer, B.; Harvey, W.L.; Haque, I.U.; Im, E.: *"On-Orbit Performance of the CloudSat EIK and Future Space Missions"*, Vacuum Electronics Conference, IVEC '07, 15-17 May 2007

[3] Bordoni, F.; Younis, M.; Varona, E.M.; Krieger, G.; "*Adaptive scan-on-receive based on spatial spectral estimation for high-resolution, wide-swath Synthetic Aperture Radar"*, IGARSS 2009, vol.1, pp.I-64-I-67, 12-17 July 2009

[4] M. Suess; B. Grafmüller, R. Zahn: *"A novel high resolution, wide swath SAR system"*, Proc. IGARSS, 2001, pp. 1013-1015, Sydney, Australia.

[5] G. Krieger; A. Moreira; H. Fiedler; I. Hajnsek; M. Werner; M. Younis; M. Zink: "*TanDEM-X: A Satellite Formation for High-Resolution SAR Interferometry*", IEEE Trans. on Geoscience and Remote Sensing, vol. 45, No. 11, December 2007.

[6] T. Strozzi, A. Wiesmann and C. Mätzler: "*Active microwave signatures of snow covers at 5.3 and 35 GHz"*, Radio Science, Vol. 32, No. 2, March 1997.

[7] Schaefer, C.; López-Dekker, P.: "*Interferometric Ka-Band SAR with DBF Capability"*, EUSAR 2012, 8-10 June 2012, Nürnberg, Germany